JOURNAL OF AGRICULTURAL AND FOOD CHEMISTRY

Article

Biological Activity and Molecular Docking Studies of Curcumin Related #, #- Unsaturated Carbonyl Based Synthetic Compounds as Anticancer Agents and Mushroom Tyrosinase Inhibitors

Syed Nasir Abbas Bukhari, Ibrahim Jantan, Oya Unsal Tan, Muhammad Sher, Naeem ul Hassan, and Hua-Li Qin

J. Agric. Food Chem., **Just Accepted Manuscript** • Publication Date (Web): 05 Jun 2014

Just Accepted

Journal of Agricultural and Food Chemistry is published by the American Chemical Society. 1155 Sixteenth Street N.W., Washington, DC 20036

Biological Activity and Molecular Docking Studies of Curcumin Related α, β-Unsaturated Carbonyl Based Synthetic Compounds as Anticancer Agents and Mushroom Tyrosinase Inhibitors

Syed Nasir Abbas Bukhari[1]*, Ibrahim Jantan[1]*, Oya Unsal Tan[2], Muhammad Sher[3], M.Naeem-ul-Hassan[3], Hua-Li Qin[4]

1. *Drug and Herbal Research Centre, Faculty of Pharmacy, Universiti Kebangsaan Malaysia, Jalan Raja Muda Abdul Aziz, 50300 Kuala Lumpur, Malaysia*
2. *Department of Pharmaceutical Chemistry, Faculty of Pharmacy, Hacettepe University, Ankara 06100, Turkey*
3. *Department of Chemistry, University of Sargodha, Sargodha 40100, Pakistan*.
4. *Department of Pharmaceutical Engineering, School of chemical engineering, Wuhan University of Technology, 205 Luoshi Road, Wuhan,430070, P.R.China.*

ABSTRACT

Hyperpigmentation in human skin and enzymatic browning in fruits which are caused by tyrosinase enzyme are not desirable. Investigations in the discovery of tyrosinase enzyme inhibitors and search for improved cytotoxic agents continue to be an important line in the drug discovery and development. In present work, a new series of thirty compounds bearing α, β-unsaturated carbonyl moiety was designed and synthesized following curcumin as model. All compounds were evaluated for their effects on human cancer cell lines and mushroom tyrosinase enzyme. Moreover, the structure-activity relationships of these compounds also explained. Molecular modeling studies of these new compounds were carried out to explore interactions with tyrosinase enzyme. Synthetic curcumin-like compounds (**2a-b)** were identified as potent anticancer agents with 81-82% cytotoxicity. Five of these newly synthesized compounds (**1a**, **8a-b**, **10a-b**), emerged to be the potent inhibitors of mushroom tyrosinase providing further insight into designing compounds useful in fields of food, health and agriculture.

KEYWORDS: Melanogenesis**,** *Curcuma Longa***,** Cytotoxicity**,** Antibrowning**,** Synthesis

INTRODUCTION

Throughout history, natural products have offered a rich source of compounds that have widespread applications in the fields of medicine, food and agriculture[1]. Structural modification of natural compounds or synthesis of new compounds, based upon designs following a natural compound scaffolding have provided us a heaps of important new commercialized drugs within the medicines, agriculture and food spheres[2, 3]. An important line in the discovery of modern anticancer drugs is exploration for enhanced cytotoxic agents principally with safety perspectives in view[4]. In line with the safety issues, plant derived natural compounds have always fascinated scientists worldwide on grounds of being biocompatible, natural compounds are deemed as potentially safe and effective skin lightening and anticancer agents[5].

Curcumin, flavonoids and numerous dietary chemo-preventive compounds have shown potential in treating cancer or dermatological disorders[6-8]. Behind cardiovascular diseases, cancer is the second principal cause of death in the world. For treating a wide range and types of cancer, plentiful effort have been started for decades but it is only recently that chemoprevention has attracted due share of attention. Combinatorial chemistry along with high-throughput screening technique directed towards molecular targets and cancer cells are well-known methods for primary anticancer drug discovery[9-11]. Curcumin is a plant-derived polyphenol obtained from *curcuma longa;* Powdered rhizome of this plant, turmeric, has been widely used for color impartment and flavoring to foods and by tradition for the treatment of various inflammatory conditions and other diseases[12-14]. Curcumin (diferuloylmethane) possesses both anticancer and antityrosinase properties[15-17].

Tyrosinase, a ubiquitous dinuclear copper enzyme, catalyzes the hydroxylation of phenols to catechols and the subsequent oxidation of catechols to quinones. This series of events take place by activation of dioxygen in the form of a side-on-bonded peroxide dicopper (II)

species, crystallographically[18] and spectroscopically identified[19, 20]. Melanin is a pigmented heteropolymer synthesized by differentiated melanocytes in specialized cellular organelles termed melanosomes. The entire process leading to the formation of melanin is called melanogenesis and is initiated with the first step of tyrosine oxidation to dopaquinone catalyzed by tyrosinase.

Melanin plays an important role in protecting human skin, from the harmful effects of UV radiation, from the sunlight. This is achieved by transfer of mature melanosomes to neighboring keratinocytes which are arranged in a supranuclear cap, protecting the DNA against incident ultraviolet light (UV) irradiation[21]. By controlling skin tone, melanin also determines the human phenotypic appearance. Although photoprotection is melanin's main function in human skin, the accumulation of an abnormal amount of melanin in specific parts of the skin resulting in more pigmented patches might become an aesthetic problem. In addition, enzymatic browning caused by tyrosinase system in fruits and fungi is undesirable in, for example, fresh fruits, beverages, vegetables, and mushrooms. In commercial or domestic processing, handling and storage of foods, tyrosinase is contemplated to have a critical role. In bruised or cut fruits, vegetables and other plant foods, tyrosinase causes enzymatic browning which subsequently leads to a significant decrease in nutritional and market values[22]. The undesirable phenomenon of hyperpigmentation in human skin and enzymatic browning in fruits have ushered researchers to seek new, enhanced and potent tyrosinase inhibitors for use in antibrowning of foods and skin whitening. Owing to the exclusively important roles in mammalian melanogenesis as well as enzymatic browning in fruits and fungi, tyrosinase inhibitors have been an important concern under the research radar for years.

Some tyrosinase inhibitors have been discovered and reviewed before[23-26]. Herein, a new series of thirty compounds bearing α, β-carbonyl moiety was designed and synthesized based on curcumin template (Figure 1) for potential use in cosmetics, clinical medicines, food industry and agriculture. Effects of synthesized compounds on human cancer cell lines and mushroom tyrosinase enzyme were evaluated. Furthermore, structure-activity relationships of synthesized compounds were also discussed.

MATERIALS AND METHODS

Materials and General Procedures

All chemicals and reagents utilized in this research were purchased from Sigma-Aldrich (St. Louis, MO, USA), Merck (Darmstadt, Germany) and Acros Organics (Geel, Belgium) of analytical grade, and were used as supplied, unless otherwise stated. A typical work-up included washing with brine and drying the organic layer with anhydrous magnesium sulfate before concentration in vacuo. ^{1}H and ^{13}C NMR spectra were recorded with a JEOL ECP spectrometer operating at 500 MHz, with Me4Si as internal standard and $CDCl_3$ or DMSO-d_6 as the solvent. High resolution mass spectra (HRMS) were determined by the Electrospray ionization mass spectrometry (ESI-MS) on MicroTOF-Q mass spectrometer (Bruker, Billerica, MA, USA). Microanalyses data were obtained from the Fison EA 1108 elemental analyzer. Infrared spectra were recorded using KBr disc on a Perkin Elmer 400 (FTIR) spectrometer. Flash column chromatography was performed with silica gel 60 (230-400mesh) (Merck) and thin layer chromatography (TLC) was carried out on pre-coated silica plates (kiesel gel 60 F_{254}, BDH). Melting points were determined on an electrothermal instrument and are uncorrected. Compounds were visualized by illumination under ultraviolet (UV) light (254 nm) or by the use of vanillin stain followed by charring on a hotplate.

Synthesis of curcumin related α, β-unsaturated carbonyl based compounds

A direct coupling approach was employed in order to synthesize α, β-unsaturated carbonyl based compounds. A general reaction proceeded by base catalyzed Claisen-Schmidt condensation, carried out by reacting a suitable aromatic aldehyde with different types of ten ketones: at a molar ratio of 1:2 for synthesizing twenty one compounds (**1a-7a**; **1b-7b**; **1c-7c**), and at a molar ratio of 1:1 for nine compounds (**8a-10a**; **8b-10b**; **8c-10c**). A general synthesis method of α, β-unsaturated carbonyl based compounds is illustrated in Figure 2. Briefly, in a single necked round bottom flask, selected aromatic aldehyde (20 mmol, 2 equivalant) and ketone (10 mmol, 1 equivalent) were mixed and dissolved in 15 mL of ethanol and stirred at 5°C for a few minutes. A 40% NaOH solution (in ethanol) was then added into the above solution drop by drop over several minutes. The mixture obtained was stirred at room temperature (27 °C) for 1-24 h. Product formation was indicated by the appearance of precipitate and change in color of the reaction mixture. TLC was used to monitor the reaction and upon completion, acidified ice was added to the mixture for quenching the reaction. Column chromatography and/or recrystallization processes were used to isolate α, β-unsaturated carbonyl based compounds.

2,6-Bis[4-(diethoxymethyl)benzylidene]cyclohexanone **(1a)**

Yellow crystals (2.59 g, 54%). mp: 112-114 ˚C; ^{1}H NMR (500 MHz, $CDCl_3$) δ: 7.89 (s, 2H), 7.29 (d, J=8Hz, 4H), 6.82 (d, J=8Hz, 4H), 5.89 (s, 2H), 3.42 (q, J=7.5, 8H), 2.32 (t, J=12.0 Hz, 4H), 1.82 (m, 2H), 1.24 (t, J=7.5, 12H); ^{13}C NMR (500 MHz, $CDCl_3$) δ: 186.4, 152.9, 144.4, 136.5, 132.5, 127.3, 126.5, 101.1, 55.0, 28.3, 27.8, 16.2 ; HRMS (ESI) m/z: 479.68 $[M+H]^+$, Microanalysis calculated for $C_{30}H_{38}O_5$ (478.62), C: 75.28%, H: 8.00%. Found C: 75.42%, H: 8.12%.

2,6-Bis-(4-dimethylamino-2-nitro-benzylidene)-cyclohexanone **(1b)**

White powder (2.78 g, 62%). mp: 139-140 ˚C; δ: 7.94 (s, 2H), 7.55 (d, J=8Hz, 2H), 7.41 (d, J=8Hz, 2H), 7.13 (s, 2H), 3.15 (s, 12H), 2.35 (t, J=12.0 Hz, 4H), 1.87 (m, 2H) ; ^{13}C NMR (500 MHz, $CDCl_3$) δ: 190.7, 149.5, 145.7, 145.6, 140.1, 128.2, 118.6, 117.6, 106.5, 46.8, 29.1, 27.5; HRMS (ESI) m/z: 451.64 $[M+H]^+$, Microanalysis calculated for $C_{24}H_{26}N_4O_5$ (450.49), C: 63.99%, H: 5.82%, N: 12.44%. Found C: 64.12%, H: 5.72%, N: 12.42%.

3,5-Bis-(4-diethoxymethyl-benzylidene)-tetrahydro-pyran-4-one **(2a)**

Pale Yellow crystals (3.06 g, 64%). mp: 106-108 ˚C; ^{1}H NMR (500 MHz, $CDCl_3$) δ: 7.85 (s, 2H), 7.32 (d, J=8Hz, 4H), 6.95 (d, J=8Hz, 4H), 5.52 (s, 2H), 3.62 (q, J=7.5, 8H), 2.69 (s, 4H), 1.18 (t, J=8, 12H); ^{13}C NMR (500 MHz, $CDCl_3$) δ: 187.2, 152.7, 143.8, 136.7, 131.9, 126.2, 125.2, 101.5, 62.4, 55.2, 16.1; HRMS (ESI) m/z: 481.65 $[M+H]^+$, Microanalysis calculated for $C_{29}H_{36}O_6$ (480.59), C: 72.48%, H: 7.55%. Found C: 72.62%, H: 7.72%.

3,5-Bis[4-(dimethylamino)2-nitro-benzylidene]-1-methyl-piperidin-4-one **(4b)**

White powder (2.56 g, 55%). mp: 181- 182 ˚C; ^{1}H NMR (500 MHz, $CDCl_3$) δ: 7.76 (s, 2H), 7.45 (d, J=8Hz, 2H), 7.23 (d, J=8Hz, 2H), 7.13 (s, 2H), 3.21 (s, 12H), 3.03 (s, 4H), 2.19 (s, 3H); ^{13}C NMR (500 MHz, $CDCl_3$) δ: 187.5, 148.9, 148.2, 143.2, 141.8, 126.7, 119.6, 118.9, 106.2, 44.5, 46.1, 38.8; HRMS (ESI) m/z: 466.72 $[M+H]^+$, Microanalysis calculated for $C_{24}H_{27}N_5O_5$ (465.50), C: 61.92%, H: 5.85%, N: 15.04%. Found C: 61.99%, H: 5.91%, N: 15.19%.

1,5-Bis-(4-diethoxymethyl-phenyl)-penta-1,4-dien-3-one **(6a)**

Pale brownish solid (1.96 g, 45%). mp: 98-100 ˚C; ^{1}H NMR (500 MHz, $CDCl_3$) δ: 7.82 (d, J=6.5Hz, 4H), 7.71 (d, J=8Hz, 2H) , 7.49 (d, J=6.5Hz, 2H), 7.16 (d, J=7Hz, 4H), 5.25 (s, 2H),

3.52 (q, J=7Hz, 8H), 1.17 (t, J=7.0, 12H); ^{13}C NMR (500 MHz, $CDCl_3$) δ: 190.5, 152.2, 148.6, 139.7, 136.4, 135.2, 132.8, 102.2, 55.5, 16.9 ; HRMS (ESI) m/z: 439.62 $[M+H]^+$, Microanalysis calculated for $C_{27}H_{34}O_5$ (438.56), C: 73.94%, H: 7.81%. Found C: 74.12%, H: 7.89%.

1,5-Bis-(4-dimethylamino-2-nitro-phenyl)-penta-1,4-dien-3-one **(6b)**

Pale yellow solid (2.97 g, 68%). mp: 177-179 ˚C; ^{1}H NMR (500 MHz, $CDCl_3$) δ: 7.70 (d, J=6Hz, 2H), 7.68 (d, J=8Hz, 2H), 7.44 (d, J=6Hz, 2H), 7.25 (d, J=8Hz, 2H), 7.12 (s, 2H), 3.15 (s, 12H); ^{13}C NMR (500 MHz, $CDCl_3$) δ: 187.5, 150.9, 148.6, 144.4, 132.8, 128.1, 117.5, 113.8, 107.9, 46.7; HRMS (ESI) m/z: 409.45 $[M-H]^+$, Microanalysis calculated for $C_{21}H_{22}N_4O_5$ (410.42), C: 61.45%, H: 5.40%, N: 13.65%. Found C: 61.48%, H: 5.62%, N: 13.77%.

2,5-Bis-(4-diethoxymethyl-benzylidene)-cyclopentanone **(7a)**

Light yellow crystals (3.12 g, 67%). mp: 88-89 ˚C; ^{1}H NMR (500 MHz, $CDCl_3$) δ: 7.69 (d, J=6.5Hz, 4H), 7.42 (s, 2H), 7.21 (d, J=6.5Hz, 4H), 5.45 (s, 2H), 3.62 (q, J=7Hz, 8H), 2.38 (t, J=7Hz, 4H), 1.22 (t, J=7.0, 12H); ^{13}C NMR (500 MHz, $CDCl_3$) δ: 189.7, 149.4, 145.5, 138.7, 136.4, 133.9, 129.1, 100.9, 56.2, 32.5, 16.1 ; HRMS (ESI) m/z: 465.72 $[M+H]^+$, Microanalysis calculated for $C_{29}H_{36}O_5$ (464.59), C: 74.97%, H: 7.81%. Found C: 75.18%, H: 7.87%.

2,5-Bis-(4-dimethylamino-2-nitro-benzylidene)-cyclopentanone **(7b)**

White powder (2.41 g, 55%). mp: 156-157 ˚C; ^{1}H NMR (500 MHz, $CDCl_3$) δ: 7.92 (d, J=6.5Hz, 2H), 7.88 (d, J=6Hz, 2H), 7.75 (d, J=6.5Hz, 2H), 7.44 (s, 2H), 3.10 (s, 12H), 2.45 (t, J=7Hz, 4H) ; ^{13}C NMR (500 MHz, $CDCl_3$) δ: 188.9, 153.2, 149.9, 144.2, 143.8, 125.8, 118.1, 116.4, 108.3, 46.9, 32.6; HRMS (ESI) m/z: 437.72 $[M+H]^+$, Microanalysis calculated for $C_{23}H_{24}N_4O_5$ (436.46), C: 63.29%, H: 5.54%, N: 12.84%. Found C: 63.42%, H: 5.48%, N: 12.72%.

2-(4-Diethoxymethyl-benzylidene)-indan-1-one **(8a)**

White powder (2.52 g, 78%). mp: 152-154 ˚C; ^{1}H NMR (500 MHz, $CDCl_3$) δ: 7.80 (d, J=8Hz, 2H), 7.69 (s, H), 7.48 (d, J=8Hz, 2H), 7.25 (d, J=7.5Hz, H), 7.20 (d, J=7.5Hz, H), 7.05 (t, J=7.5Hz, H), 6.94 (t, J=7Hz, H), 5.34 (s, H), 3.49 (q, J=7Hz, 4H), 2.75 (s, 2H), 1.29 (t, J=6Hz, 6H); ^{13}C NMR (500 MHz, $CDCl_3$) δ: 193.2, 144.5, 142.2, 140.1, 139.2, 138.8, 136.5, 130.4, 129.6, 128.1, 125.6, 125.1, 124.2, 102.2, 56.3, 29.9, 16.4 ; HRMS (ESI) m/z: 323.67 $[M+H]^+$, Microanalysis calculated for $C_{21}H_{22}O_3$ (322.40), C: 78.23%, H: 6.88%. Found C: 78.44%, H: 6.92%.

2-(4-Dimethylamino-2-nitro-benzylidene)-indan-1-one **(8b)**

Yellow semisolid (1.95 g, 63%). mp: 169-171 ˚C; ^{1}H NMR (500 MHz, $CDCl_3$) δ: 7.56 (d, J=8Hz, H), 7.48 (s, H), 7.32 (d, J=8Hz, H), 7.12 (s, H), 6.98 (d, J=7.5Hz, H), 6.91 (d, J=7.5Hz, H), 6.74 (t, J=7.5Hz, H), 6.65 (t, J=7Hz, H), 3.22 (s, 6H), 2.81 (s, 2H); ^{13}C NMR (500 MHz, $CDCl_3$) δ: 192.8, 145.6, 142.6, 141.3, 139.8, 138.2, 137.4, 130.9, 128.7, 128.0, 125.9, 123.8, 119.5, 117.6, 108.6, 46.8, 28.3 ; HRMS (ESI) m/z: 309.55 $[M+H]^+$, Microanalysis calculated for $C_{18}H_{16}N_2O_3$ (308.33), C: 70.12%, H: 5.23%, N: 9.09%. Found C: 70.18%, H: 5.59%, N: 9.18%.

2-(4-Diethoxymethyl-benzylidene)-3,4-dihydro-2H-naphthalen-1-one **(9a)**

Light yellow solid (2.67g, 80%). mp: 94-95 ˚C; ^{1}H NMR (500 MHz, $CDCl_3$) δ: 7.84 (d, J=8Hz, 2H), 7.59 (s, H), 7.47 (d, J=8.5Hz, 2H), 7.29 (d, J=7.5Hz, H), 7.22 (d, J=7.5Hz, H), 7.12 (t, J=7.5Hz, H), 7.02 (t, J=7Hz, H), 5.49 (s, H), 3.35 (q, J=7Hz, 4H), 2.29 (t, J=7Hz, 2H), 2.05 (t, J=7Hz, 2H), 1.17 (t, J=6Hz, 6H); ^{13}C NMR (500 MHz, $CDCl_3$) δ: 188.3, 152.2, 150.1, 148.5, 146.2, 143.9, 137.5, 134.4, 129.2, 127.2, 126.2, 124.8, 117.2, 101.7, 56.2, 29.5, 28.2, 16.0 ;

HRMS (ESI) m/z: 337.51 $[M+H]^+$, Microanalysis calculated for $C_{22}H_{24}O_3$ (336.42), C: 78.54%, H: 7.19%. Found C: 78.33%, H: 7.12%.

2-(4-Dimethylamino-2-nitro-benzylidene)-3,4-dihydro-2H-naphthalen-1-one **(9b)**

White powder (2.50 g, 78%). mp: 138-139 ˚C; ^{1}H NMR (500 MHz, $CDCl_3$) δ: 7.82 (d, J=6.5Hz, H), 7.57 (s, H), 7.42 (d, J=6.5Hz, H), 7.35 (s, H), 7.28 (d, J=7Hz, H), 7.20 (d, J=7Hz, H), 7.19 (t, J=7.5Hz, H), 6.92 (t, J=8Hz, H), 3.14 (s, 6H), 2.47 (t, J=7Hz, 2H), 2.14 (t, J=7Hz, 2H) ; ^{13}C NMR (500 MHz, $CDCl_3$) δ: 188.7, 152.8, 151.3, 148.9, 146.8, 144.2, 136.8, 134.6, 129.9, 127.6, 126.1, 125.3, 124.2, 107.8, 46.2, 29.9, 27.9; HRMS (ESI) m/z: 323.45 $[M+H]^+$, Microanalysis calculated for $C_{19}H_{18}N_2O_3$ (322.36), C: 70.79%, H: 5.63%, N: 8.69%. Found C: 71.12%, H: 5.52%, N: 8.72%.

2-[3-(4-Diethoxymethyl-phenyl)-acryloyl]-3,4-dihydro-2H-naphthalen-1-one **(10a)**

Yellow solid (3.16 g, 83%). mp: 121-122 ˚C; ^{1}H NMR (500 MHz, $CDCl_3$) δ: 7.75 (d, J=6Hz, H), 7.52 (d, J=6Hz, H), 7.42 (d, J=8Hz, 2H), 7.39 (d, J=8Hz, 2H), 7.32 (d, J=7Hz, H), 7.29 (d, J=7Hz, H), 7.17 (t, J=7Hz, H), 6.89 (t, J=7Hz, H), 5.29 (s, H), 3.47 (q, J=7Hz, 4H), 3.29 (t, J=8.5Hz, H), 2.12 (t, J=8Hz, 2H), 1.95 (t, J=7Hz, 2H), 1.24 (t, J=6.5Hz, 6H); ^{13}C NMR (500 MHz, $CDCl_3$) δ: 194.6, 151.1, 148.9, 144.6, 142.3, 139.2, 138.4, 136.2, 135.5, 132.4, 130.6, 129.1, 125.2, 124.2, 103.1, 66.1, 55.7, 30.2, 28.6, 16.7 ; HRMS (ESI) m/z: 379.52 $[M+H]^+$, Microanalysis calculated for $C_{24}H_{26}O_4$ (378.46), C: 76.17%, H: 6.92%. Found C: 76.21%, H: 6.91%.

2-[3-(4-Dimethylamino-2-nitro-phenyl)-acryloyl]-3,4-dihydro-2H-naphthalen-1-one **(10b)**

Pale yellow powder (2.93 g, 80%). mp: 102-103 ˚C; ^{1}H NMR (500 MHz, $CDCl_3$) δ: 7.79 (d, J=6.5Hz, H), 7.62 (d, J=6.5Hz, H), 7.45 (d, J=7.5Hz, H), 7.32 (s, H), 7.29 (d, J=7.5Hz, H), 7.21

(d, J=7.5Hz, H), 7.14 (d, J=7.5Hz, H), 7.02 (t, J=7.5Hz, H), 6.94 (t, J=7.5Hz, H), 3.45 (t, J=8.5Hz, H), 3.10 (s, 6H), 2.22 (t, J=8Hz, 2H), 2.15 (t, J=8Hz, 2H) ; ^{13}C NMR (500 MHz, $CDCl_3$) δ: 193.8, 152.2, 148.7, 145.2, 142.8, 139.6, 137.1, 136.8, 135.6, 131.9, 130.5, 129.4, 124.8, 123.5, 116.5, 106.2, 65.8, 46.8, 31.3, 28.7 ; HRMS (ESI) m/z: 365.55 $[M+H]^+$, Microanalysis calculated for $C_{21}H_{20}N_2O_4$ (364.39), C: 69.22%, H: 5.53%, N: 7.69%. Found C: 69.34%, H: 5.59%, N: 7.81%.4

MTT assay

MTT assay was performed for determining the effect of synthetic compounds on normal (MCF-10A) mammary epithelial cells. MCF-10A cells were maintained in Dulbecco's modified Eagle's medium/Ham's F-12 medium (1:1) with 10% foetal calf serum, 2 mM glutamine, insulin (10 µg/mL), hydrocortisone (500 ng/mL), and epidermal growth factor (20 ng/mL). Cells were passaged every 2 to 3 days using trypsin EDTA (ethylenediaminetetraacetic acid). MCF-10A cells were plated at a density of 10^4 cells per millilitre in 96-well flat-bottomed plates. After 24 hours, the medium was carefully aspirated and tested compounds (curcumin analogues) were added in quadruplicate in 200 µL of medium to give a final concentration of not more than 0.1% (v/v) dimethylsulfoxide (DMSO). The cells were then permitted to grow for 96 hours at 37°C. The medium was removed and fresh medium with MTT (3-[4,5-dimethylthiazol-2-yl]-2,5-diphenyltetrazolium bromide) (0.4 mg/mL) was added to each well for 3 hours. All medium was aspirated and the formazan product generated by viable cells was solubilised with 150 µL of DMSO. Plates were vortexed and the absorbance at 540 nm determined using a microplate reader. Results were expressed as the percentage inhibition of proliferation compared to controls containing 0.1% DMSO.

Anticancer activity

For determining the anticancer activity a propidium iodide (PI) fluorescence assay was performed on MCF-7 (breast cancer cell line), PC-3 (prostate cancer cell line), HL-60 (promyelocytic leukemia cell line), H-460 (lung cancer cell line) and HT-29 (colon cancer cell line) cell lines[27]. Propidium iodide (PI), a dye which binds to DNA, provides a rapid and accurate means for quantitating total nuclear DNA. The principle of this assay is based on the fact that PI is not able to penetrate an intact cell membrane and the fluorescence signal intensity of the PI is directly proportional to the amount of DNA in each cell. So the cells which have damaged membranes or altered permemability profiles are scored as dead cells. For a typical PI cytotoxicity assay, cells, after trypsinization and counting, were seeded at 3000-7500 cells/well in 200 µl media in sterile tissue culture grade 96 well plates and allowed to recover for 24 h in humidified 5% CO_2 incubator at 37 °C. After this, compounds (in 0.1% DMSO) were added onto triplicate wells with 10 µM concentrations. 0.1% DMSO alone was used as control. Treatment with test compounds was continued for 48 h. After completion of designated treatment period, the medium was removed and cells were treated with 25 µl of propidium iodide (50 µg/mL in water/medium) per well. The above plates with samples were frozen at -80 °C for 24 h, then thawed and allowed to equilibrate to room temperature. Plates were read on a fluorometer (Polar-Star BMG Tech), using 530 nm excitation and 620 nm emission wavelength. Lastly, percent cytotoxicity of the compounds was calculated by using following formula:

$$\% \text{ Cytotoxicity} = \frac{A_C - A_{TC}}{A_C} \times 100$$

Where A_C= Absorbance reading of control and A_{TC}= Absorbance reading of treated cells. The results were compared with the standard drug inhibitors flavopiridol (0.5µM).

Tyrosinase assay

The spectrophotometric assay for tyrosinase was performed according to the reported method with slight modifications[28]. Briefly, L-DOPA was used as substrate to screen the synthesized compounds for the diphenolase inhibitory activity of tyrosinase. Positive controls in the assay were Kojic acid and 4-Butylresorcinol. 2% stock solutions of compounds were prepared in DMSO and diluted using phosphate buffer (pH = 6.8). These synthesized compounds were pre-incubated in 50 mM phosphate buffer (pH = 6.8) at 25 °C for 10 min with thirty units of mushroom tyrosinase (0.5 mg/mL). L-DOPA (0.5 mM) was then added to the reaction mixture. Reaction was monitored by following formation of L-DOPA chrome for 1 min measured by the change in absorbance at 475 nm. Triplicate measurements were taken for each concentration and average was used for further calculations. Dose-response curves were interpolated to obtain the IC_{50} values.

Molecular modeling

Molecular modeling studies were performed with MOE (The Molecular Operating Environment) Version 2011.10, software available from Chemical Computing Group Inc., 1010 Sherbrooke Street West, Suite 910, Montreal, Canada H3A2R7, http://www.chemcomp.com. The ligands were built using the builder tool of the MOE program and subjected to energy minimization (MMFF94x, gradient: 0.05). The X-ray crystallographic structure of mushroom tyrosinase (PDB: 2Y9W) [29] was obtained from the Protein Data Bank. The errors of the protein were corrected by the *Structure Preparation* process in MOE. After correction, hydrogens were added and partial charges (Gasteiger methodology) were calculated. Site finder application was used to detect the possible binding pocket. The default Triangle Matcher placement method was applied for docking. GBVI/WSA dG scoring function which estimates the free energy of binding of the

ligand from a given pose was used to rank the final poses. The ligand-enzyme complexes with lowest *S* score were selected for each ligand.

Statistical analysis

Analysis was carried out using a complete randomized design and treatments were run in triplicates (n = 3). Statistical analysis was done using analysis of variance (ANOVA) method of general linear model (GLM) procedure using SAS V8 (Cary, NC, USA) for multiple comparisons. $P < 0.05$ was considered to be statistically significant.

RESULTS AND DISCUSSION

Chemistry

Claisen-Schmidt condensation was used for the synthesis of the desired α, β-unsaturated carbonyl based compounds[30] by reacting different ketones and the appropriate aryl aldehyde. Twenty one compounds (**1a-7a**; **1b-7b**; **1c-7c)** were synthesized in presence of NaOH at a 1:2 molar ratio in ethanol while some compounds were synthesized in acetic acid by passing dry HCl gas through the mixture. Claisen-Schmidt condensation was also employed to synthesize nine compounds (**8a-10a**; **8b-10b**; **8c-10c**) similar to chalcone analogues however employing 1:1 molar ratio of ketone and aldehyde (Figure 2). Both types of catalytic systems, i.e., NaOH and dry HCl gas mixture, were used to synthesize eight compounds (**7a**, **8a**, **10a**, **7b**, **8b**, **10b**, **7c**, **8c**). Catalytic system employing HCl gas mixture gave high percentage yields compared to NaOH. Using NaOH as a catalyst resulted in producing mixture of several different unidentified products necessitating excessive purification using column chromatography.

Spectrophotometric techniques were used to characterize the synthesized compounds. An elemental analysis of C, H, and N, and melting points are represented. Representative carbon nuclear magnetic resonance spectra were also recorded. NH absorptions were not seen in the ^{1}H

NMR spectra of the compounds **4a**, **4b** and **4c**, it has previously been shown by other researchers[30, 31].

Cytotoxicity towards MCF-10A normal mammary epithelial cells

The rule of three, relating to activity-exposure-toxicity, presents the single most difficult challenge in the design and advancement of drug candidates to the development stage. Absorption, distribution, metabolism and excretion (ADME) studies are widely used in drug discovery to optimize this balance of properties necessary to convert lead compounds into drugs that are both safe and effective for human patients[32]. Therefore, in vitro cell viability assay was performed by using the MCF-10A that is a normal cell line and was used as a comparison. MCF-10A cells were treated with synthetic compounds for 96 hours and cell viability was measured using the MTT assay. Results are expressed in terms of percentage of toxicity (Table 1). The compounds were found to be nontoxic and majority of compounds showed more than 95% cell viability. Therefore, the compounds are biologically safe and can be used as the therapeutic agent for future drug discovery study.

Effects on Human Cancer Cell Lines

Anticancer activity of curcumin is one of the most widely explored activities among numerous others like anti-inflammatory activity. In vitro cytotoxicity assays performed in various cell lines originating from different organs show that curcumin have beneficial effects in, including but not limited to,; prostate cancer cells[33], ovarian cancer cells[34], gastric carcinoma cells[35], liver cancer cells, hepatocel- lular carcinoma cells[36], cervical cancer cells[37], breast cancer cells[38], colon cancer cells[39], lung carcinoma cell[40], bladder cancer cells[41] and pancreatic adenocarcinoma cell[42]. This provides strong preliminary data for the justification of clinical studies in humans.

Synthesized compounds were tested in present investigation for their capacity to inhibit the growth of five different cancer cell lines (PC-3, MCF-7, HL-60, H-460 and HT-29). Compound **2b** was found to have highest anticancer activity inhibiting 82% of PC-3 cells; this was closely followed by compound **2a** showing 81% inhibition. These two compounds also show similarly comparative levels of anticancer activity (75 - 82%) on the other four cell lines used for experiments. Compound **2a** and **2b** were followed by six curcumin-like compounds (**2a-b**, **3a-b** and **4a-b**) which had promising anti cancer activity (59 - 82%) (Figure 3). This was followed by twelve compounds (**1a-c**, **2c**, **3c**, **4c**, **5a-b**, **6a-b** and **10a-b**) which show moderate effect (40 - 58%). Insignificant activity was shown by remaining compounds. For the anticancer activity experiments positive control used was flavopiridol which show 79% inhibition of H-460 cells at 0.5μM concentration. Generally, curcumin like compounds show similar inhibitory anticancer activity on the tested cell lines and it was observed that the average difference in inhibitory activities was not more than 5% types of tested cancer cell lines. For most active compounds (**2a**, **2b**, **4a** and **4b**) the median inhibition concentration (IC_{50}) was calculated using GraphPad Prism software (GraphPad Software, San Diego, CA, USA) and it was observed that compound **2b** was very potent anticancer agent among all other tested compounds with very low IC_{50} value in the range of 1.04 to 1.08 μM (Table 2).

Compounds **2a**, **2b**, **4a** and **4b** were found to have high potency against different types of cancer cell lines. It can be depicted from their physicochemical properties (Table 2) that these compounds have potential to be new lead compounds in developing anticancer agents. Physicochemical properties of tested compounds were found within optimal range (Molecular weight <500; clog*P* <5 and TPSA <140)[43, 44].

Effects on the Diphenolase Activity of Mushroom Tyrosinase

Tyrosinase inhibitory assay was performed for all synthesized curcumin-related compounds by measuring the oxidation of L-DOPA as previously reported[28]**.** A concentration-dependent enzyme activity inhibition by the compounds was observed. It was observed that the activity of remaining enzyme swiftly decreased when the concentration of compound (inhibitor) was increased. Table 1 summarizes the enzyme inhibition data expressed as IC_{50}. The majority of synthetic curcumin related compounds (**1a-c**, **2a-c**, **3a-b**, **6a-c**, **7a-c**, **8a-c**, **9a-c**, **10a-c**) exhibit <100 μM inhibitory activities against mushroom tyrosinase. With IC_{50} ranging from 5.34 to 10.11 μM, five compounds (**1a**, **8a-b** and **10a-b**) exhibited promising tyrosinase inhibitiory activity better than positive control Kojic acid (10.93μM). Two of the synthesized compounds (**8a** and **10a)**, with diethoxymethyl group at position 4, were found to be the strongest inhibitors among all tested compounds with IC_{50} values 6.83μM and 5.34μM respectively.

Structure-activity relationship analysis

It was observed that the presence or absence of groups on the two aromatic rings and the linker between the two aromatic rings both played key roles in determining the anticancer inhibitory activity of the various analogs on the tested cancer cells. From their data for SAR of mono-carbonyl analogues, the research group of G Liang, had shown previously that acetone and cyclohexanone spacers are much more favorable than the cyclopentanone one[45] for enhanced anticancer activity. Conclusion drawn by Liang's group is also afforded by present study as all synthetic compounds containing cyclopentanone ring system (**7a-7c**) have lesser anticancer activity when compared to compounds with acetone and cyclohexanone system. In fact, among these three group of compounds (**1, 6, 7**), compounds bearing cyclohexanone were found to be most active.

Different activity trends were observed among the different series of curcumin-related compounds when either linear or cyclic linkers were used between the two aromatic rings of curcumin related compounds. In general, tetrahydropyran-4-one (**2a-c**) linker containing compounds exhibited the strongest activities, moderate activity was exhibited by compounds with *N*-Methyl-4-piperidone (**3a-c**), while three compounds (**4a-c**) with 4-piperidone showed good inhibition power however it was lesser compared to compounds bearing *N*-Methyl-4-piperidone. Bis-derivatives, bearing either 1-Benzyl-4-piperidone (**5a-c**), acetone (**6a-c**) or cyclopentanone (**7a-c**) linker, were less active compared to the rest. Conversely, among the mono-derivatives (**8-10**), merely compounds bearing di-carbonyl linker (**10a-b**) were shown to have moderate growth inhibitory anticancer activity in the tested cell lines.

Presence of a heteroatom linker in groups of compounds (**2**, **3**, **4**) resulted in enhanced anticancer activities compared to the compounds without a heteroatom linker (**1**, **6**, **7**). This finding suggests that flexibility of curcumin-like compounds could improve their anticancer activities which could be due to the ease of interactions with the DNA of cancer cells. Contrary to this, compounds with small and rigid linker would be less active due to the difficulty of interactions with DNA. Association of curcumin flexibility with curcumin-DNA interaction which could be a possible explanation for antitumor activity is a valuable and interesting finding[46, 47].

Effects of substitution of various groups curcumin related compound activity were compared. It was observed that introduction of 2-nitro-4-dimethylamine combination on the aromatic rings improved anticancer activity of curcumin related compounds. In all the three groups (based on substitution pattern **a**, **b**, **c**), compounds bearing combination of 2-nitro and 4-dimethylamine show exceptionally elevated anticancer activity whereas presence of

diethoxymethyl group at position 4 of rings consequently produces markedly reduced anticancer activity. Further, presence of pyrrolidine at position 4 of compounds (**1-10c**) results in compounds which are not highly active.

Analysis of the effects of curcumin related compounds on tyrosinase activity produced structure-activity relationship with new and interesting findings. Based upon different substituted groups, with two exception (**4b** and **7b** more active than **4a** and **7a**), it was observed that compounds having diethoxymethyl group at position 4 of rings (group **a**) were most active against the mushroom tyrosinase activity. Like the anticancer activity, substitution of pyrrolidine at position 4 of compounds (**1-10c**) did not produce strongly active compounds for tyrosinase inhibition. An interesting finding was the presence of di-carbonyl group (**10a-b**) that resulted in maximum tyrosinase inhibition even better than the positive controls. In general, the mono-derivatives (**8-10**) show better anti-tyrosinase activity as compared to bis-derivatives (**2-7**). However presence of a heteroatom linker (**2**, **3**, and **4**) didn't result in compounds with a better antityrosinase activity when compared to those without a heteroatom linker (**1**, **6**, and **7**).

Molecular Docking Study

Tyrosinase enzyme has binuclear copper binding site and tropolone and kojic acid bind the entrance of this site[29, 48]. In this study, Site Finder application in MOE was used to find the possible binding sites in the enzyme. The region consisting of S1 and S2 site was indicated as active pocket (Figure 4). S1 contains binuclear copper binding site where S2 locates near the entrance of this site.

To simplify, docking results were evaluated in groups. First of all, **(a)** the docking results of compound **1-7a** (bis-derivatives) which have different keton structures were considered. Compound **1a** and **6a** gave the same orientation (Figure 5) while the others oriented in a different

426 way. It was seen that Val283 and His244 hold **1a** and **6a** at the entrance of copper binding site by
427 H-arene interaction of the phenyl rings of both compounds (Figure 6). Furthermore, C=O moiety
428 of compounds **1a** and **6a** might form a weak hydrogen bond with backbone NH of His85 (about
429 4Å). Also, nonpolar part of cyclohexanone of compound **1a** made hydrophobic interactions with
430 Val283 (less than 3Å). Because of the hindrance of nonpolar part of Val283, synthetic
431 compounds **2a-5a** and **7a** might be oriented in a different way. **(b)** The orientations of **8a-10a**
432 **(**mono-derivatives) occurred similar to that of bis-derivatives (except **9a**) by their interactions
433 with Val283, His244 and His85 (Figure 6). **(c)** Compounds carrying pyrrolidine moiety **(1-10c)**,
434 were oriented so that C=O groups of the compounds located close to NH of Asn81 instead of
435 His85. Substitution of pyrrolidine might decrease the flexibilities of these compounds at the
436 entrance, which might cause a reduction in the activity.

437 To conclude, ten series containing thirty novel α, β-unsaturated carbonyl based curcumin
438 related compounds were successfully synthesized using the Claisen-Schmidt condensation
439 reaction. All synthesized compounds were analyzed for anticancer and antityrosinase activity.
440 Compounds **2a-b** were identified as potent anticancer agents with 81-82% inhibition of cancer
441 cell lines. Five of these compounds (**1a**, **8a-b**, **10a-b**), emerged to be the potent inhibitors of
442 Mushroom tyrosinase. Molecular modeling studies were also performed to see the interactions of
443 synthetic compounds with X-ray crystallographic structure of mushroom tyrosinase. It also
444 provided further insight into designing compounds with structural features that may translate into
445 higher activity. Our studies have established that these curcumin-like compounds, with
446 appropriate structural modifications, have the potential to be developed as anticancer agents for
447 humans and can also be further studied for use in medicines, cosmetic products, food industry as

well as agricultural purposes. Further studies are required for use and development of these synthetic compounds in food and agricultural field as antibrowning agents.

ABBREVIATIONS USED

PI, Propidium iodide; DMSO, Dimethyl sulfoxide; L-DOPA, L-3, 4-dihydroxyphenylalanine; MOE, Molecular operating environment; TPSA, Topological polar surface area.

ACKNOWLEDGEMENTS

Dr. Syed Nasir Abbas Bukhari thanks University Kebangsaan Malaysia for postdoctoral contract.

FUNDING

This research was supported by University Kebangsaan Malaysia (Grants no.: UKM-DLP-2013-013).

AUTHOR INFORMATION

Corresponding Author

*E-mail: (SNAB) snab@pharmacy.ukm.my; snabphd@yahoo.com; snab_hussaini@yahoo.com (IJ) ibj@pharmacy.ukm.my

CONFLICT OF INTEREST

The authors declare no competing financial interest.

References

471 1. Dias, D. A.; Urban, S.; Roessner, U., A Historical Overview of Natural Products in Drug
472 Discovery. *Metabolites* **2012**, *2*, 303-336.
473 2. Guo, Z. R., [Modification of natural products for drug discovery]. *Yao xue xue bao* =
474 *Acta pharmaceutica Sinica* **2012**, *47*, 144-57.
475 3. Valli, M.; Pivatto, M.; Danuello, A.; Castro-Gamboa, I.; Silva, D. H. S.; Cavalheiro, A.
476 J.; Araújo, Â. R.; Furlan, M.; Lopes, M. N.; Bolzani, V. d. S., Tropical biodiversity: has it been a
477 potential source of secondary metabolites useful for medicinal chemistry? *Química Nova* **2012**,
478 *35*, 2278-2287.
479 4. Bhatnagar, I.; Kim, S. K., Marine antitumor drugs: status, shortfalls and strategies.
480 *Marine drugs* **2010**, *8*, 2702-20.
481 5. Prakash, O.; Kumar, A.; Kumar, P.; Ajeet, A., Anticancer Potential of Plants and Natural
482 Products: A Review. *American Journal of Pharmacological Sciences* **2013**, *1*, 104-115.
483 6. Brown, A.; Shi, Q.; Moore, T. W.; Yoon, Y.; Prussia, A.; Maddox, C.; Liotta, D. C.;
484 Shim, H.; Snyder, J. P., Monocarbonyl Curcumin Analogues: Heterocyclic Pleiotropic Kinase
485 Inhibitors That Mediate Anticancer Properties. *Journal of Medicinal Chemistry* **2013**, *56*, 3456-
486 3466.
487 7. Gupta, A. K.; Gover, M. D.; Nouri, K.; Taylor, S., The treatment of melasma: A review
488 of clinical trials. *Journal of the American Academy of Dermatology* **2006**, *55*, 1048-1065.
489 8. Shakibaei, M.; Buhrmann, C.; Kraehe, P.; Shayan, P.; Lueders, C.; Goel, A., Curcumin
490 Chemosensitizes 5-Fluorouracil Resistant MMR-Deficient Human Colon Cancer Cells in High
491 Density Cultures. *PLoS ONE* **2014**, *9*, e85397.
492 9. Lu, W.; Ogasawara, M. A.; Huang, P., Models of reactive oxygen species in cancer. *Drug*
493 *discovery today. Disease models* **2007**, *4*, 67-73.

494 10. Rao, Y. K.; Fang, S.-H.; Tzeng, Y.-M., Differential effects of synthesized 2′-oxygenated
495 chalcone derivatives: modulation of human cell cycle phase distribution. *Bioorganic &*
496 *Medicinal Chemistry* **2004**, *12*, 2679-2686.
497 11. Buolamwini, J. K., Novel anticancer drug discovery. *Current Opinion in Chemical*
498 *Biology* **1999**, *3*, 500-509.
499 12. Shoji, M.; Nakagawa, K.; Watanabe, A.; Tsuduki, T.; Yamada, T.; Kuwahara, S.;
500 Kimura, F.; Miyazawa, T., Comparison of the effects of curcumin and curcumin glucuronide in
501 human hepatocellular carcinoma HepG2 cells. *Food Chemistry* **2014**, *151*, 126-132.
502 13. Vaughan, R. A.; Garcia-Smith, R.; Dorsey, J.; Griffith, J. K.; Bisoffi, M.; Trujillo, K. A.,
503 Tumor necrosis factor alpha induces Warburg-like metabolism and is reversed by anti-
504 inflammatory curcumin in breast epithelial cells. *International Journal of Cancer* **2013**, *133*,
505 2504-2510.
506 14. Basnet, P.; Skalko-Basnet, N., Curcumin: An Anti-Inflammatory Molecule from a Curry
507 Spice on the Path to Cancer Treatment. *Molecules* **2011**, *16*, 4567-4598.
508 15. Hosoya, T.; Nakata, A.; Yamasaki, F.; Abas, F.; Shaari, K.; Lajis, N.; Morita, H.,
509 Curcumin-like diarylpentanoid analogues as melanogenesis inhibitors. *J Nat Med* **2012**, *66*, 166-
510 176.
511 16. Lee, K.-H.; Ab. Aziz, F. H.; Syahida, A.; Abas, F.; Shaari, K.; Israf, D. A.; Lajis, N. H.,
512 Synthesis and biological evaluation of curcumin-like diarylpentanoid analogues for anti-
513 inflammatory, antioxidant and anti-tyrosinase activities. *European Journal of Medicinal*
514 *Chemistry* **2009**, *44*, 3195-3200.

17. Youssef, D.; Nichols, C. E.; Cameron, T. S.; Balzarini, J.; De Clercq, E.; Jha, A., Design, synthesis, and cytostatic activity of novel cyclic curcumin analogues. *Bioorganic & Medicinal Chemistry Letters* **2007**, *17*, 5624-5629.

18. Matoba, Y.; Kumagai, T.; Yamamoto, A.; Yoshitsu, H.; Sugiyama, M., Crystallographic evidence that the dinuclear copper center of tyrosinase is flexible during catalysis. *The Journal of biological chemistry* **2006**, *281*, 8981-90.

19. Solomon, E. I.; Sundaram, U. M.; Machonkin, T. E., Multicopper Oxidases and Oxygenases. *Chemical Reviews* **1996**, *96*, 2563-2606.

20. Rolff, M.; Schottenheim, J.; Decker, H.; Tuczek, F., Copper-O2 reactivity of tyrosinase models towards external monophenolic substrates: molecular mechanism and comparison with the enzyme. *Chemical Society Reviews* **2011**, *40*, 4077-4098.

21. Park, H. Y.; Kosmadaki, M.; Yaar, M.; Gilchrest, B. A., Cellular mechanisms regulating human melanogenesis. *Cell. Mol. Life Sci.* **2009**, *66*, 1493-1506.

22. Artés, F.; Castañer, M.; Gil, M. I., Revisión: El pardeamiento enzimático en frutas y hortalizas mínimamente procesadas Review: Enzymatic browning in minimally processed fruit and vegetables. *Food Science and Technology International* **1998**, *4*, 377-389.

23. Jiménez, M.; Chazarra, S.; Escribano, J.; Cabanes, J.; García-Carmona, F., Competitive Inhibition of Mushroom Tyrosinase by 4-Substituted Benzaldehydes. *Journal of Agricultural and Food Chemistry* **2001**, *49*, 4060-4063.

24. Kubo, I.; Kinst-Hori, I., Flavonols from Saffron Flower: Tyrosinase Inhibitory Activity and Inhibition Mechanism†. *Journal of Agricultural and Food Chemistry* **1999**, *47*, 4121-4125.

536 25. Okombi, S.; Rival, D.; Bonnet, S.; Mariotte, A.-M.; Perrier, E.; Boumendjel, A.,
537 Discovery of Benzylidenebenzofuran-3(2H)-one (Aurones) as Inhibitors of Tyrosinase Derived
538 from Human Melanocytes. *Journal of Medicinal Chemistry* **2005**, *49*, 329-333.
539 26. Parvez, S.; Kang, M.; Chung, H.-S.; Bae, H., Naturally occurring tyrosinase inhibitors:
540 mechanism and applications in skin health, cosmetics and agriculture industries. *Phytotherapy*
541 *Research* **2007**, *21*, 805-816.
542 27. Dengler, W. A.; Schulte, J.; Berger, D. P.; Mertelsmann, R.; Fiebig, H. H., Development
543 of a propidium iodide fluorescence assay for proliferation and cytotoxicity assays. *Anti-cancer*
544 *drugs* **1995**, *6*, 522-32.
545 28. Bao, K.; Dai, Y.; Zhu, Z.-B.; Tu, F.-J.; Zhang, W.-G.; Yao, X.-S., Design and synthesis
546 of biphenyl derivatives as mushroom tyrosinase inhibitors. *Bioorganic & Medicinal Chemistry*
547 **2010**, *18*, 6708-6714.
548 29. Ismaya, W. T.; Rozeboom, H. t. J.; Weijn, A.; Mes, J. J.; Fusetti, F.; Wichers, H. J.;
549 Dijkstra, B. W., Crystal Structure of Agaricus bisporus Mushroom Tyrosinase: Identity of the
550 Tetramer Subunits and Interaction with Tropolone. *Biochemistry* **2011**, *50*, 5477-5486.
551 30. Dimmock, J. R.; Padmanilayam, M. P.; Puthucode, R. N.; Nazarali, A. J.; Motaganahalli,
552 N. L.; Zello, G. A.; Quail, J. W.; Oloo, E. O.; Kraatz, H.-B.; Prisciak, J. S.; Allen, T. M.; Santos,
553 C. L.; Balzarini, J.; De Clercq, E.; Manavathu, E. K., A Conformational and Structure−Activity
554 Relationship Study of Cytotoxic 3,5-Bis(arylidene)-4-piperidones and Related N-Acryloyl
555 Analogues. *Journal of Medicinal Chemistry* **2001**, *44*, 586-593.
556 31. Das, U.; Alcorn, J.; Shrivastav, A.; Sharma, R. K.; De Clercq, E.; Balzarini, J.; Dimmock,
557 J. R., Design, synthesis and cytotoxic properties of novel 1-[4-(2-

558 alkylaminoethoxy)phenylcarbonyl]-3,5-bis(arylidene)-4-piperidones and related compounds.
559 *European Journal of Medicinal Chemistry* **2007**, *42*, 71-80.
560 32. Nassar, A.-E. F.; Kamel, A. M.; Clarimont, C., Improvingthe decision-making process in
561 structural modification of drug candidates: reducing toxicity. *Drug Discovery Today* **2004**, *9*,
562 1055-1064.
563 33. Hour, T.-C.; Chen, J.; Huang, C.-Y.; Guan, J.-Y.; Lu, S.-H.; Pu, Y.-S., Curcumin
564 enhances cytotoxicity of chemotherapeutic agents in prostate cancer cells by inducing
565 p21WAF1/CIP1 and C/EBPβ expressions and suppressing NF-κB activation. *The Prostate* **2002**,
566 *51*, 211-218.
567 34. Chan, M. M.; Fong, D.; Soprano, K. J.; Holmes, W. F.; Heverling, H., Inhibition of
568 growth and sensitization to cisplatin-mediated killing of ovarian cancer cells by polyphenolic
569 chemopreventive agents. *Journal of Cellular Physiology* **2003**, *194*, 63-70.
570 35. Koo, J. Y.; Kim, H. J.; Jung, K. O.; Park, K. Y., Curcumin inhibits the growth of AGS
571 human gastric carcinoma cells in vitro and shows synergism with 5-fluorouracil. *Journal of*
572 *medicinal food* **2004**, *7*, 117-21.
573 36. Notarbartolo, M.; Poma, P.; Perri, D.; Dusonchet, L.; Cervello, M.; D'Alessandro, N.,
574 Antitumor effects of curcumin, alone or in combination with cisplatin or doxorubicin, on human
575 hepatic cancer cells. Analysis of their possible relationship to changes in NF-kB activation levels
576 and in IAP gene expression. *Cancer Letters* **2005**, *224*, 53-65.
577 37. Bava, S. V.; Puliappadamba, V. T.; Deepti, A.; Nair, A.; Karunagaran, D.; Anto, R. J.,
578 Sensitization of taxol-induced apoptosis by curcumin involves down-regulation of nuclear factor-
579 kappaB and the serine/threonine kinase Akt and is independent of tubulin polymerization. *The*
580 *Journal of biological chemistry* **2005**, *280*, 6301-8.

581 38. Aggarwal, B. B.; Shishodia, S.; Takada, Y.; Banerjee, S.; Newman, R. A.; Bueso-Ramos,
582 C. E.; Price, J. E., Curcumin suppresses the paclitaxel-induced nuclear factor-kappaB pathway in
583 breast cancer cells and inhibits lung metastasis of human breast cancer in nude mice. *Clinical*
584 *cancer research : an official journal of the American Association for Cancer Research* **2005**, *11*,
585 7490-8.
586 39. Lev-Ari, S.; Strier, L.; Kazanov, D.; Madar-Shapiro, L.; Dvory-Sobol, H.; Pinchuk, I.;
587 Marian, B.; Lichtenberg, D.; Arber, N., Celecoxib and curcumin synergistically inhibit the
588 growth of colorectal cancer cells. *Clinical cancer research : an official journal of the American*
589 *Association for Cancer Research* **2005**, *11*, 6738-44.
590 40. Sen, S.; Sharma, H.; Singh, N., Curcumin enhances Vinorelbine mediated apoptosis in
591 NSCLC cells by the mitochondrial pathway. *Biochemical and Biophysical Research*
592 *Communications* **2005**, *331*, 1245-1252.
593 41. Kamat, A. M.; Sethi, G.; Aggarwal, B. B., Curcumin potentiates the apoptotic effects of
594 chemotherapeutic agents and cytokines through down-regulation of nuclear factor-kappaB and
595 nuclear factor-kappaB-regulated gene products in IFN-alpha-sensitive and IFN-alpha-resistant
596 human bladder cancer cells. *Molecular cancer therapeutics* **2007**, *6*, 1022-30.
597 42. Lev-Ari, S.; Vexler, A.; Starr, A.; Ashkenazy-Voghera, M.; Greif, J.; Aderka, D.; Ben-
598 Yosef, R., Curcumin Augments Gemcitabine Cytotoxic Effect on Pancreatic Adenocarcinoma
599 Cell Lines. *Cancer Investigation* **2007**, *25*, 411-418.
600 43. Lipinski, C. A.; Lombardo, F.; Dominy, B. W.; Feeney, P. J., Experimental and
601 computational approaches to estimate solubility and permeability in drug discovery and
602 development settings. *Advanced Drug Delivery Reviews* **2001**, *46*, 3-26.

44. Ertl, P.; Rohde, B.; Selzer, P., Fast Calculation of Molecular Polar Surface Area as a Sum of Fragment-Based Contributions and Its Application to the Prediction of Drug Transport Properties. *Journal of Medicinal Chemistry* **2000**, *43*, 3714-3717.

45. Liang, G.; Shao, L.; Wang, Y.; Zhao, C.; Chu, Y.; Xiao, J.; Zhao, Y.; Li, X.; Yang, S., Exploration and synthesis of curcumin analogues with improved structural stability both in vitro and in vivo as cytotoxic agents. *Bioorganic & Medicinal Chemistry* **2009**, *17*, 2623-2631.

46. Zsila, F.; Bikadi, Z.; Simonyi, M., Circular dichroism spectroscopic studies reveal pH dependent binding of curcumin in the minor groove of natural and synthetic nucleic acids. *Organic & Biomolecular Chemistry* **2004**, *2*, 2902-2910.

47. Caruso, F.; Rossi, M.; Benson, A.; Opazo, C.; Freedman, D.; Monti, E.; Gariboldi, M. B.; Shaulky, J.; Marchetti, F.; Pettinari, R.; Pettinari, C., Ruthenium–Arene Complexes of Curcumin: X-Ray and Density Functional Theory Structure, Synthesis, and Spectroscopic Characterization, in Vitro Antitumor Activity, and DNA Docking Studies of (p-Cymene)Ru(curcuminato)chloro. *Journal of Medicinal Chemistry* **2011**, *55*, 1072-1081.

48. Sendovski, M.; Kanteev, M.; Ben-Yosef, V. S.; Adir, N.; Fishman, A., First Structures of an Active Bacterial Tyrosinase Reveal Copper Plasticity. *Journal of Molecular Biology* **2011**, *405*, 227-237.

FIGURE CAPTIONS

Figure 1: Chemical modifications in structure of curcumin.

Figure 2: Synthesis of curcumin related α, β-unsaturated carbonyl based compounds, Reagents and conditions: (i) NaOH, EtOH, Room temperature.

Figure 3: Percentage cytotoxicity of selected curcumin like synthetic compounds against various cancer cell lines.

Figure 4: Binuclear copper binding site (S1) and its entrance (S2) region of mushroom tyrosinase enzyme.

Figure 5: Superimposition of the best poses of compound **1a**, **6a**, **8a** and **10a** (**1a**, **6a**, **8a** and **10a** are shown as yellow, blue, pink and green respectively).

Figure 6: The orientations of compound **1a** in tyrosinase active site (**1a** and residues are shown as yellow and blue respectively).

Table 1: Anticancer activity and inhibitory effects of synthetic curcumin like compounds against mushroom tyrosinase.

Compounds	Anticancer activity (%)						Tyrosinase inhibitory activity (IC_{50} µM)
	HT-29	PC-3	MCF-7	H-460	HL-60	MCF-10A	
1a	55	56	59	52	60	0	10.11
1b	59	58	62	64	61	4	14.21
1c	42	40	41	48	45	0	45.66
2a	79	81	77	78	75	7	32.21
2b	81	82	79	80	80	12	36.23
2c	47	46	42	48	47	5	125.48
3a	69	64	61	61	59	2	51.82
3b	71	60	63	62	59	6	55.22
3c	59	51	52	55	53	5	>200
4a	72	71	70	71	69	9	66.32
4b	73	75	72	74	71	11	18.12
4c	31	32	45	31	30	0	>200
5a	41	41	40	43	44	0	102.44
5b	42	44	45	45	46	0	122.24
5c	21	22	22	20	21	0	ND
6a	42	43	41	42	40	0	11.04
6b	44	47	46	46	47	5	11.45
6c	12	11	13	15	15	0	77.83
7a	33	32	34	32	32	0	27.87
7b	35	36	35	38	39	0	23.22
7c	21	24	24	26	25	0	99.43
8a	12	14	13	13	15	0	06.83
8b	15	16	16	18	18	0	8.12
8c	09	11	15	12	16	0	45.84
9a	22	24	23	25	22	0	21.17
9b	25	26	26	27	25	0	26.22
9c	11	06	09	12	17	0	77.88
10a	47	45	46	44	43	4	5.34
10b	55	56	55	58	55	0	7.13
10c	23	26	28	21	20	2	56.76
Flavopiridol*	77	70	72	79	74	-	-
4-Butylresorcinol	-	-	-	-	-	-	33.16
Kojic acid	-	-	-	-	-	-	10.93

* 0.5µM concentration

HT-29 (colon cancer cell line): PC-3 (prostate cancer cell line): MCF-7 (breast cancer cell line): H-460 (lung cancer cell line): HL-60 (promyelocytic leukemia cell line): MCF-10A (normal mammary epithelial cell line).

675 **Table 2:** Physicochemical Properties and cytotoxicity of most active compounds **2a**, **2b**, **4a** and
676 **4b** against human cancer cell lines.
677

Com.	Anticancer activity IC_{50} (μM)					Physicochemical Properties[1]			
	HT-29	PC-3	MCF-7	H-460	HL-60	Clog*P*[*]	TPSA[**]	H-b(d)[#]	H-b(a)[##]
2a	2.39±0.27	2.31±0.62	2.42±0.93	2.40±0.22	2.45±0.12	5.23	63.24	0	6
2b	1.06±0.59	1.04±0.42	1.08±0.45	1.06±0.41	1.05±0.48	3.52	124.42	0	10
4a	2.79±0.75	2.82±0.11	2.81±0.32	2.87±0.59	2.85±0.52	4.68	66.03	1	6
4b	2.72±0.19	2.69±0.64	2.63±0.34	2.70±0.74	2.77±0.18	2.97	127.22	1	10

678 [1] Calculated with Molinspiration property engine v.2013.09 (http://www.molinspiration.com).
679 [*]Calculated log *P* (molecular hydrophobicity); [**] Topological polar surface area of the molecules
680 [#] H-bond donors; [##] H-bond acceptors

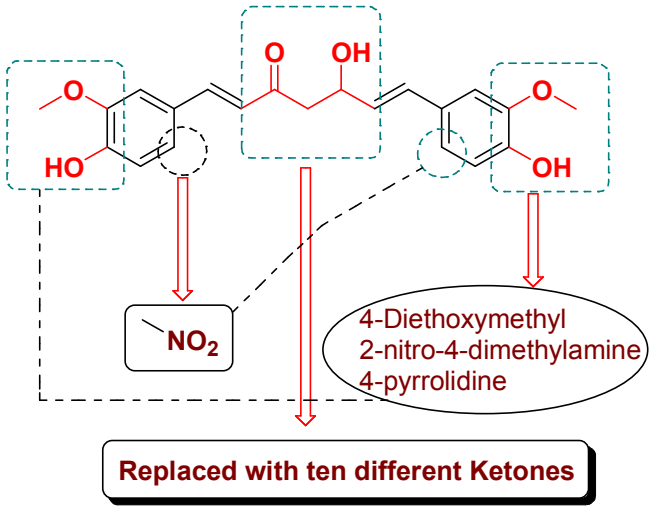

Figure 1: Chemical modifications in structure of curcumin

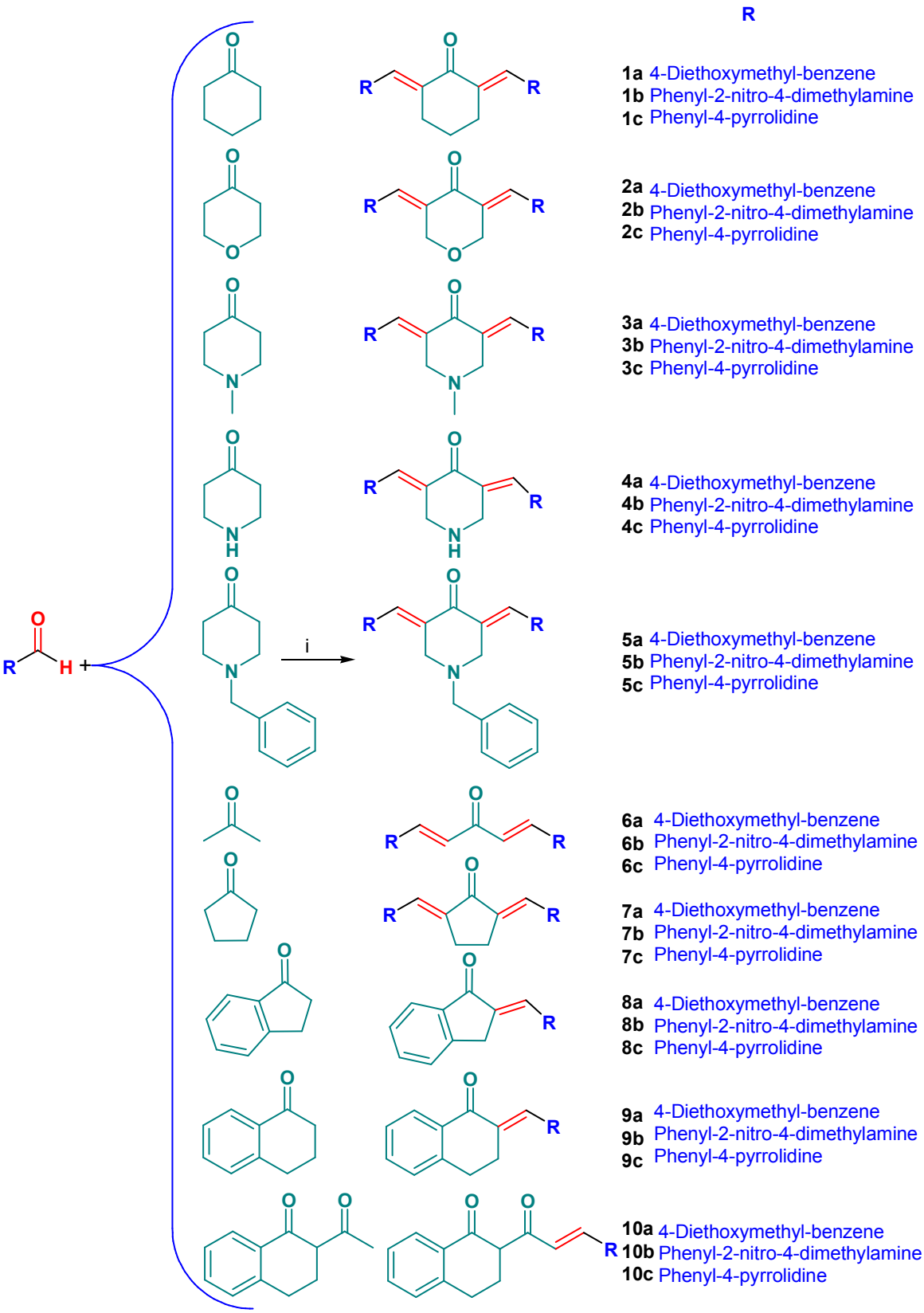

Figure 2: Synthesis of curcumin related α, β-unsaturated carbonyl based compounds, Reagents and conditions: (i) NaOH, EtOH, Room temperature.

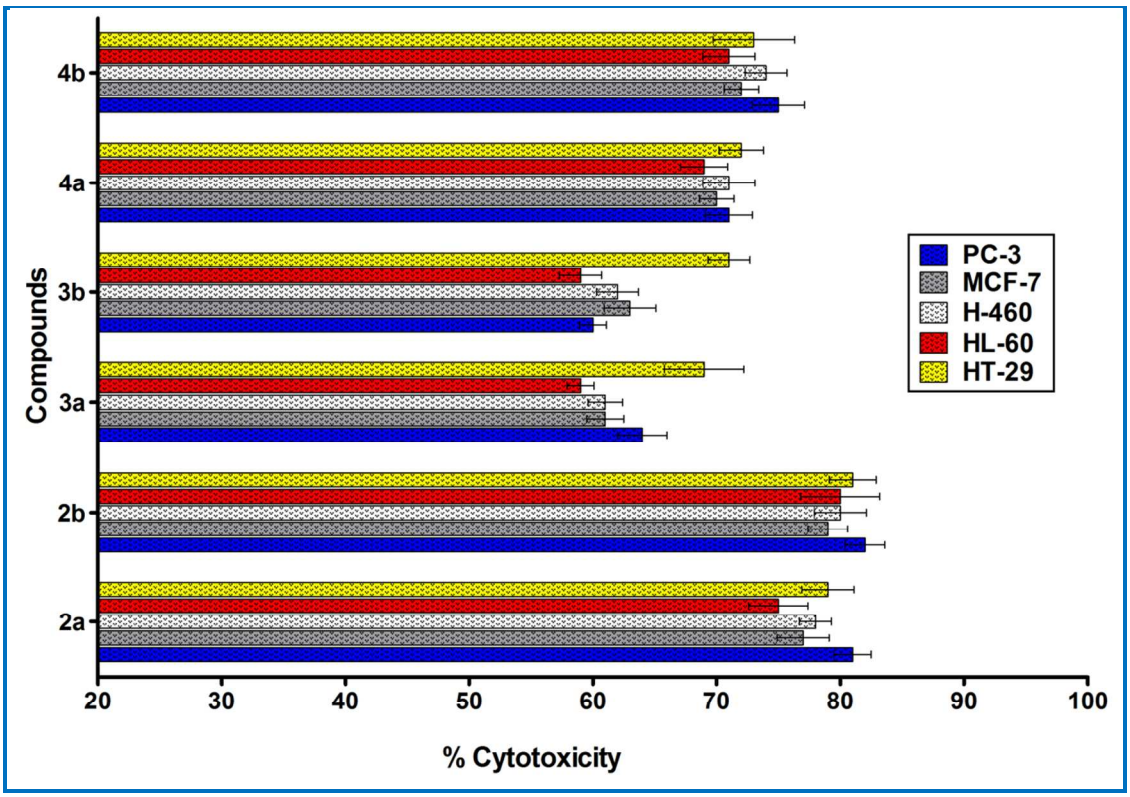

Figure 3: Percentage cytotoxicity of selected curcumin like synthetic compounds against various cancer cell lines.

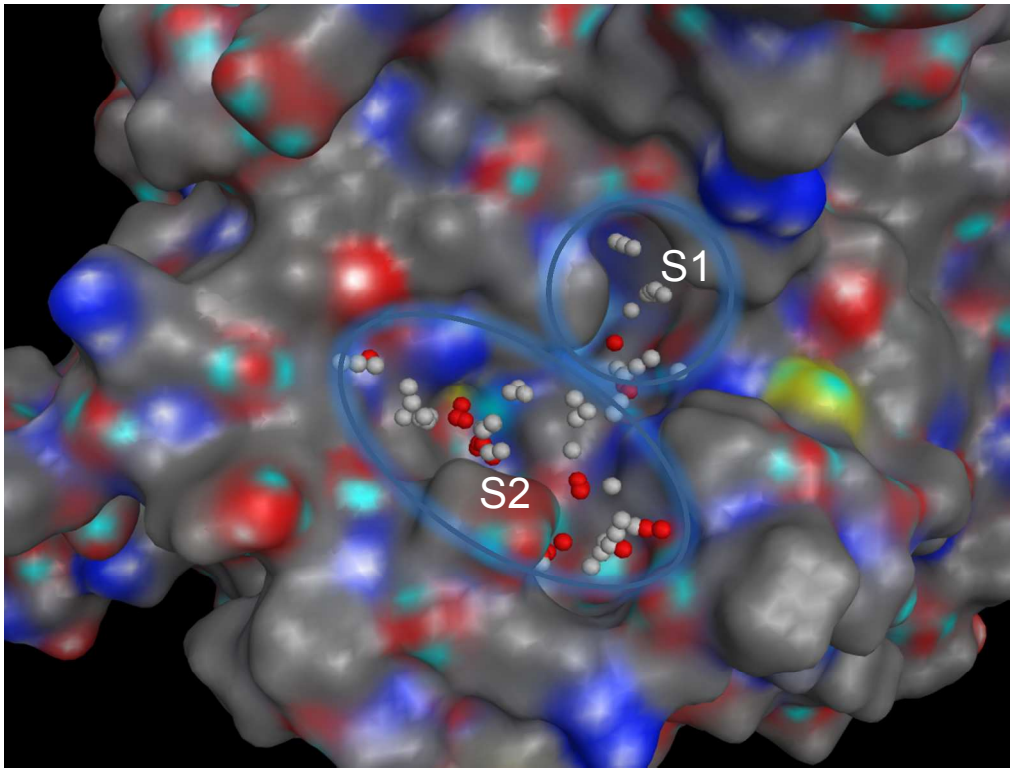

Figure 4: Binuclear copper binding site (S1) and its entrance (S2) region of mushroom tyrosinase enzyme.

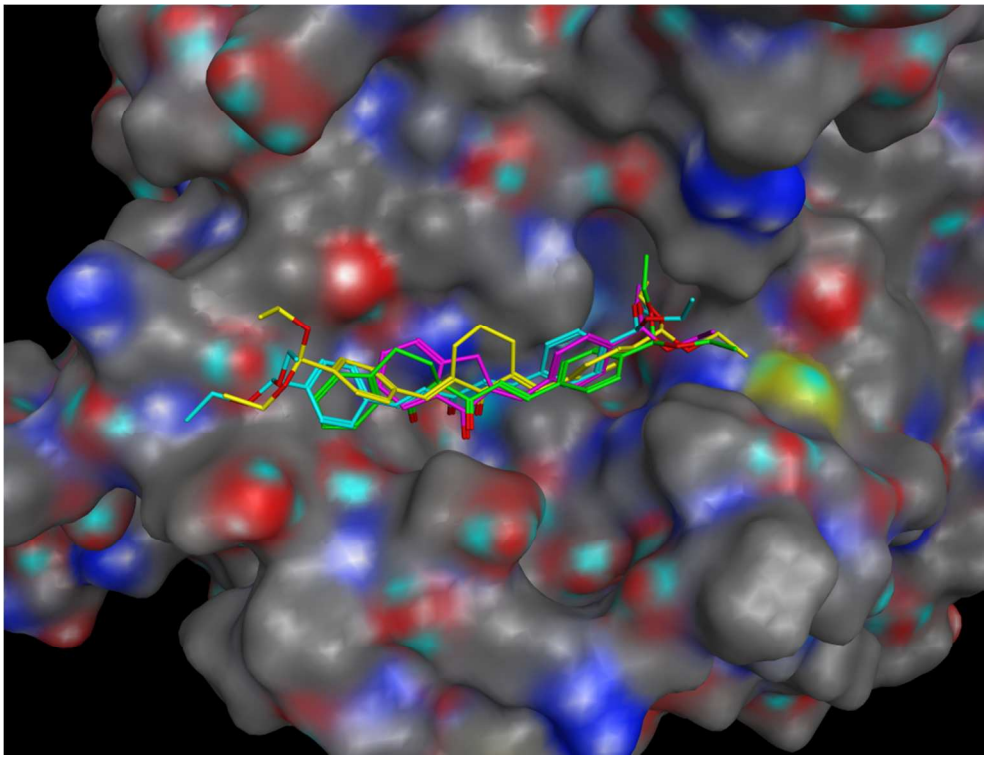

Figure 5: Superimposition of the best poses of compound **1a**, **6a**, **8a** and **10a** (**1a**, **6a**, **8a** and **10a** are shown as yellow, blue, pink and green respectively).

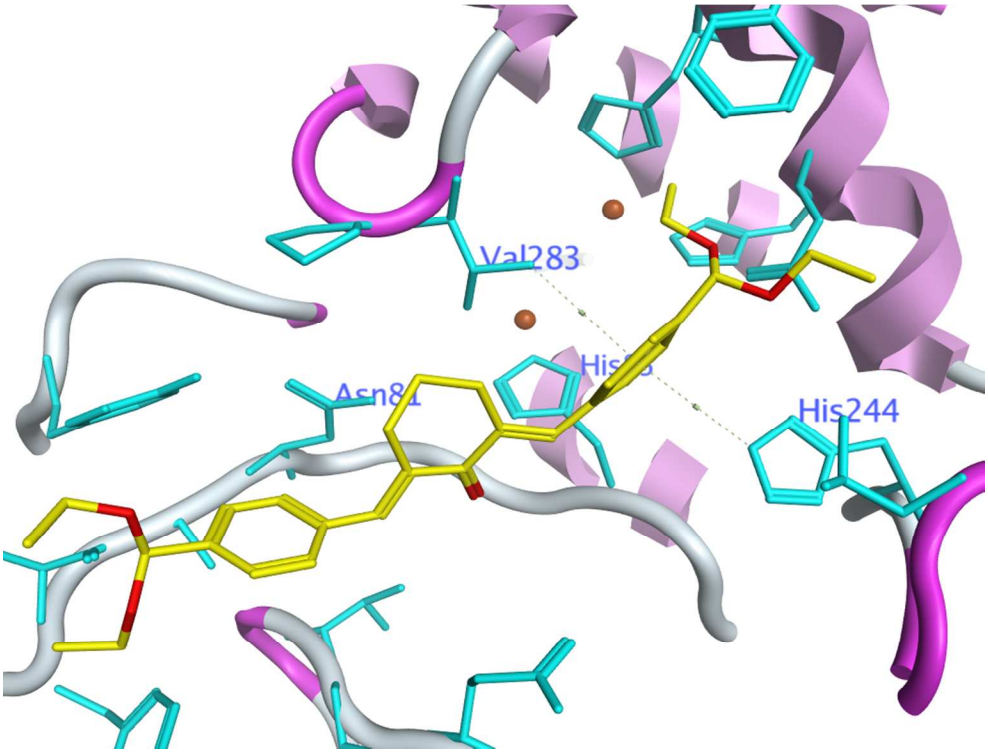

Figure 6: The orientations of compound **1a** in tyrosinase active site (**1a** and residues are shown as yellow and blue respectively)

GRAPHIC FOR TABLE OF CONTENTS